Achieving the Most Stringent CO2 Commercial Truck Standards with Opposed Piston Engine

Dr. Gerhard Regner – Vice President, Performance and Emission

Fabien Redon - Vice President, Technology Development

John Koszewnik, Chief Technical Officer

Laurence Fromm – Vice President, Business and Strategy Development

Zoltan Bako – Director, Application Engineering

Abstract

With the passage of Euro 6, and the recent U.S. introduction of new CO_2 limits for heavy-duty trucks and buses, vehicle and engine manufacturers are facing a daunting challenge [1]. Compliance with these regulations requires significant financial investments in new technologies, all designed to increase fuel efficiency while decreasing emissions. But, to remain competitive, manufacturers cannot pass along these costs to fleet owners.

One solution to this problem is the opposed-piston engine. This engine, which has been optimized by Achates Power, was once widely used in a variety of applications including aviation, maritime and military vehicles. After overcoming the architecture's historical challenges, the Achates Power opposed-piston engine now delivers a step-wise improvement in brake thermal efficiency over the most advanced conventional four-stroke engines. In addition, with the elimination of parts such as the cylinder head and valve train, it is also less complex and less costly to produce—making it even more appealing to manufacturers.

After a brief overview of the opposed-piston architecture's inherent efficiency benefits, this technical paper features detailed performance and emissions results of a multi-cylinder Achates Power opposed-piston engine configured to meet current commercial truck requirements. Presented for the first time in Europe, these results demonstrate the engine's ability to:

- Significantly improve fuel efficiency over the best diesel engines in the same class
- Comply with Euro 6/U.S. 2010 emissions standards

The discussion also includes an in-depth analysis of the opposed-piston, multi-cylinder test engine's indicated thermal efficiency, friction and pumping losses as well as a road map for achieving 47.6 percent best-point brake thermal efficiency (BTE), which translates to 46.6 percent cycle-weighted BTE on medium duty engine, while the same technology results 51.5% best point BTE, and 50.4% cycle weighted BTE on a heavy duty engine. Furthermore, the technical paper provides a vibration analysis between the Achates Power opposed-piston architecture and the inline six-cylinder, four-stroke engine, which dominates the medium- and heavy-duty truck market.

Opposed-Piston Engine Architectural Advantages

Opposed-piston, two-stroke engines were conceived in the 1800s in Europe and subsequently developed in multiple countries for a wide variety of applications, including aircraft, ships, tanks, trucks and locomotives. They maintained their presence throughout the twentieth century. An excellent summary of the history of opposed-piston engines can be found in the SAE book, *Opposed-Piston Engines: Evolution, Use, and Future Applications* by M. Flint and J.P. Pirault [2]. Produced initially for their manufacturability and high power density, opposed-piston, two-stroke engines have demonstrated superior fuel efficiency compared to their four-stroke counterparts. This section examines the underlying reasons for the superior fuel efficiency and emissions. The OP2S diesel engine has the following efficiency advantages compared to a conventional, four-stroke diesel engine:

1. Reduced Heat Losses

The Achates Power opposed-piston engine, which includes two pistons facing each other in the same cylinder, offers the opportunity to combine the stroke of both pistons to increase the effective stroke-to-bore ratio of the cylinder working volume.

For example, when coupling two piston trains from a conventional, single-piston engine with a stroke-to-bore ratio of 1.1, the resulting opposed-piston engine bore-to-stroke ratio is twice or 2.2. This can be accomplished while preserving the engine and piston speed of the base design.

To achieve the same stroke-to-bore ratio with a single-piston engine, the mean piston speed would double for the same engine speed. This would severely limit the engine speed range and, therefore, the power output.

The increase in stroke-to-bore ratio has a direct mathematical relationship to the area-to-volume ratio of the combustion space. For example, when comparing a single-piston engine to an opposed-piston engine with the same piston and crank dimensions, the following outcome can be seen:

	Single Piston	**OP2S**
Trapped Volume/Cyl.	1.0L	1.6L
Bore	102.6 mm	102.6 mm
Total Stroke	112.9 mm	224.2 mm
Stroke-to-Bore Ratio	1.1	2.2
Compression Ratio	15:01	15:01
Surface Area (Min Vol.)	20 cm^2	20 cm^2
Volume (Min Vol.)	71 cm^3	114 cm^3
Area-to-Volume Ratio	0.28	0.18

Table 1 OP2S compared to a single-piston engine.

In this example, the reduction in the surface area top volume ratio is a very significant 36%. The lower surface area directly leads to a reduction in heat transfer.

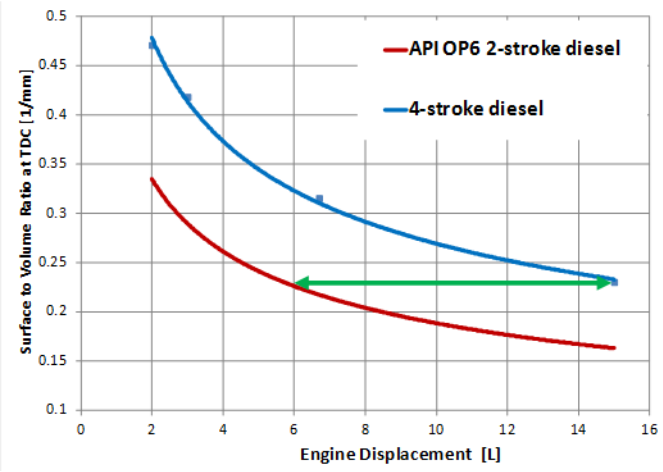

Figure 1 Surface-to-volume ratio versus engine displacement for an OP2S and conventional engine.

Figure 1shows that the area-to-volume ratio of a six-liter, opposed-piston engine is equivalent to a 15-liter, conventional diesel engine. This reduction in area-to-volume ratio is one of the main reasons why larger displacement engines are more efficient than smaller ones. With the Achates Power opposed-piston architecture, there is the opportunity to achieve the efficiency of much larger engines.
An additional benefit of the reduced heat losses in the opposed-piston engine, especially for commercial vehicles, is the reduction in fan power and radiator size, further contributing to vehicle level fuel savings.

2. Leaner Combustion

When configuring an opposed-piston, two-stroke engine of the same displacement as a four-stroke engine –f or example, converting a six-cylinder, conventional engine into a three-cylinder, opposed-piston engine – the power that each cylinder has to deliver is the same. The opposed-piston engine fires each of the three cylinders at each revolution while the four-stroke engine fires each of its six cylinders one out of two revolutions.

Therefore, the amount of fuel injected for each combustion event is similar, but the cylinder volume is more than 50% greater for the Achates Power opposed-piston engine. So for the same boost conditions, the opposed-piston engine will achieve leaner combustion, which increases the ratio of specific heat. Increasing the ratio of specific heat increases the pressure rise during combustion and increases the work extraction per unit of volume expansion during the expansion stroke.

Ideal Engine Efficiency

$$\eta_{ideal} = 1 - \frac{1}{r_c^{\gamma-1}}$$

r_c = compression ratio

γ = ratio of specific heats

3. Faster and Earlier Combustion at the Same Pressure Rise Rate

The larger combustion volume for the given amount of energy released also enables shorter combustion duration while preserving the same maximum pressure rise rate. The faster combustion improves thermal efficiency by reaching a condition closer to constant volume combustion. The lower heat losses as described above lead to a 50% burn location closer to the minimum volume. Figure 2 illustrates how the heat release rate compares between a four-stroke engine and the Achates Power opposed-piston engine.

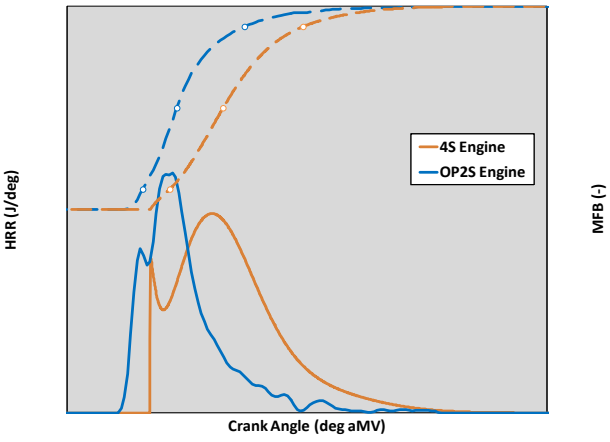

Figure 2: Heat release rate comparison between a four stroke and the OP2S.

The ideal combustion should occur at the minimum volume and be instantaneous. The opposed-piston engine is much closer to this ideal condition at the same pressure rise rate.

The aforementioned fundamental OP2S thermal efficiency advantages [3] are further amplified by:

- Lower heat loss due to higher wall temperature of the two piston crowns compared to a cylinder head. (Reduced temperature delta).
- Reduced pumping work thanks to uniflow scavenging with the OP2S architecture giving higher effective flow area than a comparable four-stroke or a single-piston, two-stroke uniflow or loop-scavenged engine [4].
- A decoupled pumping process from the piston motion due to the two-stroke architecture allows alignment of the engine operation with a maximum compressor efficiency line [5].
- Lower NOx characteristics as a result of lower BMEP requirements because of the two-stroke cycle operation [6].

Efficiency and Emissions Enablers

Combustion System

Achates Power has developed a proprietary combustion system [7] composed of two identical pistons coming together to form an elongated ellipsoidal combustion volume where the injectors are located at the end of the long axis [8] (Figure 3).

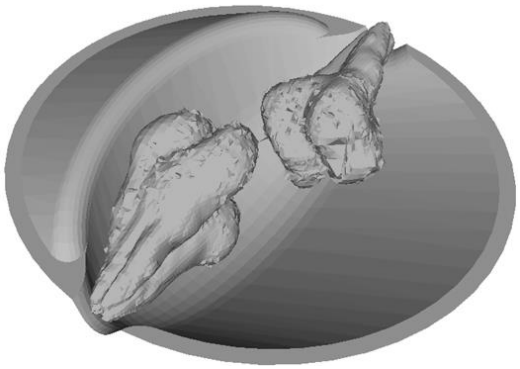

Figure 3: Schematic of the combustion system with plumes coming out of two side-mounted injectors

This combustion system allows:

- High turbulence, mixing and air utilization with both swirl and tumble charge motion as is illustrated below with the high turbulent kinetic energy available at the time of auto ignition
- Ellipsoidal combustion chamber resulting in air entrainment into the spray plumes from two sides
- Inter-digitated, mid-cylinder penetration of fuel plumes enabling larger λ=1 iso-surfaces
- Excellent control at lower fuel flow rates because of two small injectors instead of a single higher flow rate
- Multiple injection events and optimization flexibility with strategies such as injector staggering and rate-shaping [8]

The result is no direct fuel spray impingement on the piston walls and minimal flame-wall interaction during combustion. This improves performance and emissions [9] with fewer hot spots on the piston surfaces to further reduce heat losses [8].

Air System

To provide a sufficient amount of air for combustion, two-stroke engines need to maintain an appropriate pressure difference between the intake and exhaust ports (i.e. to scavenge exhaust out of the cylinder after combustion and push in fresh air mass).

For applications that require the engine to change speed and load in a transient manner, such as automotive applications, external means of air pumping are required. Among the various possible configurations of the air system with turbocharger and supercharger combinations, the layout as described in Figure 4 is the preferred configuration [10].

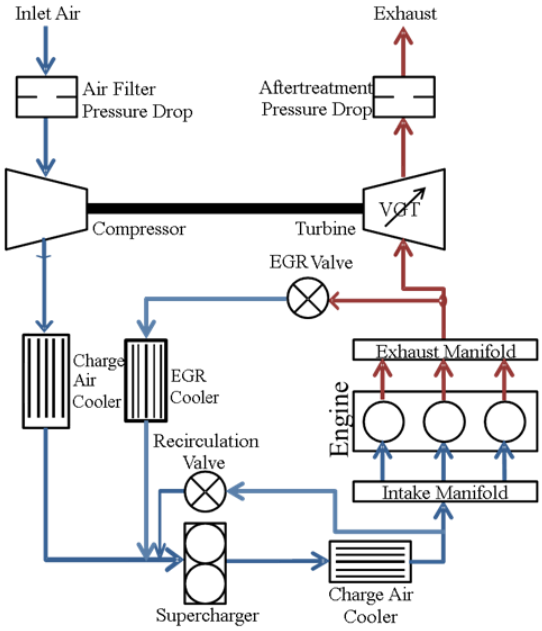

Figure 4: Opposed-piston, two-stroke preferred air system layout.

Advantages of such an air system are summarized as follows:

- The compressor provides high pressure before the supercharger, which is multiplied by the supercharger. This means low supercharger pressure ratios are sufficient for high intake manifold density, reducing pumping work.
- The maximum required compressor pressure ratio is lower compared to regular turbo-only air systems of four-stroke engines.
- The use of a supercharger recirculation valve allows greater control of the flow through the engine, thus providing flexibility for precise control of boost, scavenging ratio, and trapped residuals to minimize pumping work and NOx formation across the engine map
- Lowering the flow through the engine by decreasing the pressure difference across the engine reduces the pumping penalty at low load points. This, together with having no dedicated intake and exhaust stroke for moving mass from and to the cylinder improves BSFC.
- The supercharger and recirculation valve improves transient response [11].
- Accurate control of the engine pressure differential provides very good cold start and catalyst light off capabilities [12] . For similar reasons, exhaust gas temperatures and catalyst light-off can be maintained during low load and idle conditions.
- Low-speed torque is increased by selecting the appropriate gear ratios on the supercharger [9].
- Drive EGR with a supercharger reduces the required pumping work [9].
- Cool air and EGR together reduces fouling of the coolers [9][13].

Multi-Cylinder Research Engine Description

OP Engine Engineering Challenges

Historically, two-stroke, opposed-piston engines are known to have fuel efficiency advantages, but have faced several engineering challenges that have kept them from going mainstream. The Achates Power created a robust engine that satisfies the performance, emissions and durability standards of the 21st century. The primary challenges that Achates Power had to overcome include finding an effective way to reduce oil consumption, increase piston compression ring life, manage the thermal loads on the piston and liner, and support 200+ bar cylinder pressures at the wrist pin.

The oil control strategy in a two-stroke engine is different than in a four-stroke due to the ports in the cylinder liner, which also impact the piston ring wear. If there is not enough lubricant on the liner, the ring life deteriorates. If there is too much oil, consumption increases. Two-stroke engine has a firing event every crankshaft revolution whereas a four-stroke has a firing event every two revolutions. Inherently, the two-stroke lacks the intake stroke which, for a four-stroke engine, allows for additional cooling of the piston and cylinder liner. Creative solutions are required to sufficiently cool the piston and cylinder liner. Traditionally, two-strokes have had limitations with wrist pin life at peak cylinder pressures above 150 bar. This again is primarily driven by the lack of an intake stroke where inertia overcomes the cylinder pressure and lifts the piston from the wrist pin and creating a void to be filled with oil.

Single-Cylinder Development Engine

After focusing on the optimal engine architecture, Achates Power developed its single-cylinder variant, designated the A48-1. These single-cylinder engines have been used for performance and emissions development and have provided a platform for mechanical system technology development.

Achates Power utilized creative, but proven, solutions to overcome the presented engineering challenges. In the case of oil consumption and ring life the focus was on liner honing techniques, piston ring material and coating. This resulted in oil consumption that is on par with four-stroke engines in the medium- and heavy-duty industry.

Improving liner and piston thermal management required a combined effort balancing heat in and out of the liner and piston. On the hot side, combustion variables must be controlled while care must be taken to avoid hot spots from the fuel plume flame fronts. The cold side of both the liner and piston uses targeted cooling solutions to cool critical areas. Achates Power has utilized its proprietary real-time piston and liner temperature measurement system to gain a fundamental understanding and control of thermal issues.

Overcoming the 150 bar peak cylinder pressure limit of the typical two-stroke was accomplished by introducing the bi-axial wrist pin. This offset bearing is fixed to the connecting rod, which forces the opposing journals to lift as it articulates. This has successfully allowed Achates Power to achieve 220 bar peak cylinder pressure.

The combustion has been optimized for both fuel efficiency and emissions. Achates Power utilizes unique combustion bowl shapes that allow for optimal mixing and scavenging by inducing additional tumble in the combustion chamber. The piston shapes were designed as a system with the fuel injectors, cylinder ports, crankshaft-to-crankshaft phasing and compression ratio.

After resolving these engineering challenges and achieving industry-leading fuel efficiency based on the single-cylinder testing, it was time to prove these results carry over into a multi-cylinder design. Up until this point, simulation and computational models were used to transfer results from a single-cylinder to a multi-cylinder. Missing were cylinder-to-cylinder interactions with the air charge system and the scaling of overall engine friction. At this point, Achates Power designed and built the three-cylinder A48-3-16.

Multi-Cylinder Modular Development Engine

The A48-3-16 shares most of the power cylinder with the A48-1 and in an effort to reduce the development schedule, many components are compatible. Similar to the A48-1, the A48-3-16 is designed for a peak cylinder pressure of 200 bar with overload conditions of 220 bar. The block was cast from compacted graphite iron (CGI).

The A48-1 was oriented with the cylinder axis in the horizontal plane while the A48-3-16 is oriented vertically. The drive toward a vertical engine is based on customers' preferences for packaging in a vehicle.

The A48-1 and A48-3-16 engines were created as a research test bed to quickly iterate through multiple different designs. In creating such a platform, some compromises were made versus how a production engine would be conceived. Some examples of the experimental aspects include:

- Higher overall engine mass – robustness and quick turn around
- Larger package size – modular/swappable components
- Off-the-self air system components – supercharger, turbocharger and coolers, not tuned for the engine
- Higher friction
    - Oversized off-the-shelf connecting rod big end and main bearings

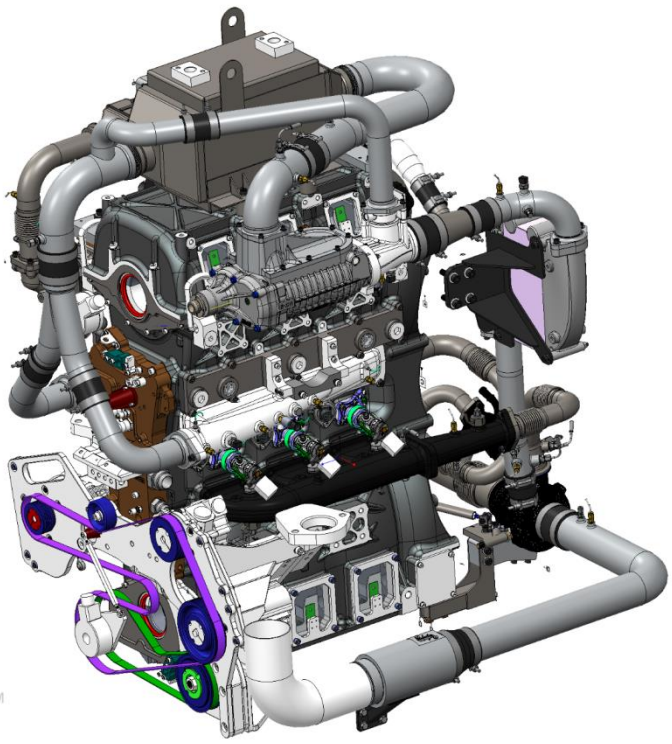

Figure 5: A48-3-16 Front and Rear View

    - Aftermarket oil and coolant pumps
    - Remote mounted gearbox with redundant bearings causing over constraint
    - Dual dry sump scavenging pumps and air-oil separators
- Modular gearbox connecting the exhaust and intake crank
- Modular FEAD
- Modular accessories

Friction can be trimmed in several areas. Due to available bearing sizes and the need for a robust development platform, the loading calculations for both the connecting rod big end and main bearings resulted in oversized components. More of the cooling in the opposed-piston engine is done with the oil so the efficiency of the oil pump is important and can be improved with deeper supplier involvement. The gearbox, which connects the intake and exhaust crankshaft, is carried over and compatible with the single cylinder A48-1. This gearbox was also designed with significant margins for robustness at the expense of friction and fuel efficiency.

Purpose-Built Multi-Cylinder

Many of these aspects of the engine allow for quicker and more productive development cycles. With a purpose-built engine and known boundary conditions, the fuel efficiency can be further improved. By removing the need for modular systems, the mass and packaging space can be dramatically improved. The learnings from this modular A48-3-16 are used to design the next-generation application-specific engines for volume production.

Engine Power and Torque Targets

The engine was configured to meet the following torque curve. The 4.9L three-cylinder engine has a peak power output of 275hp@2200 RPM and a peak torque of 1100Nm from 1200 to 1600 RPM (Table 3)

The air and EGR system was sized to achieve EGR and air-fuel ratio levels suitable to comply with U.S. 2010 emissions levels when coupled with conventional SCR and DPF aftertreatment.

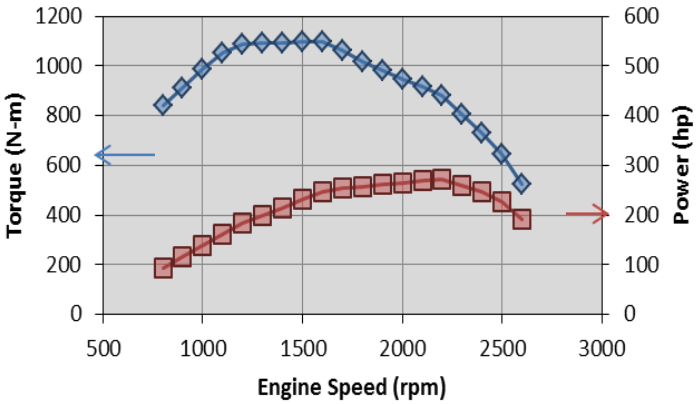

Figure 6: A48-3-16 engine specification and power and torque curves

A48-3-16 engine specification	
Displacement	4.9 L
Arrangement, # of Cyl.	Inline 3
Bore	98.4 mm
Total Stroke	215.9 mm
Stroke-to-Bore Ratio	2.2
Compression Ratio	15:01
Nominal Power (kW@rpm)	205 @ 2200
Max. Torque (Nm@rpm)	1100 @ 1200-1600

Engine Build

The engine build team worked for approximately two months to deliver the A48-3-16engine to the test group. During this time, all components were verified for form, fit and function. Critical dimensions and clearances were recorded for use during engine inspections and to monitor component wear. To meet the aggressive schedule, the procurement of components was planned so assembly could begin while waiting for subsequent systems. The power cylinder and block were assembled first, followed by the fuel, coolant, air charge systems and finally the FEAD. The engine was then instrumented and connected to the test cell. The engine was first run on fuel eleven months after the initiation of the project.

Figure 7: Engine components

Engine Testing - Instrumentation

In-cylinder pressure is measured at 0.5° crank-angle intervals with three AVL GH14D Select piezoelectric pressure transducers coupled to Kistler 5064 charge amplifiers. The cylinder pressure signal is pegged to an average of the intake and exhaust manifold pressures during scavenging, measured with Kistler 4005B and 4045A high-speed pressure transducers, respectively. Custom in-house software is used to acquire and process the crank-angle based data.

Exhaust emissions are measured with an FTIR in conjunction with a California Analytical Instruments (CAI) emissions analyzer. These are used to measure the steady-state concentration of five exhaust species (CO2, CO, O2, HC, NOx) and intake CO2. An AVL 483 Micro Soot Sensor provides a measure of exhaust soot content in real time. A Davinci DALOC is used for real-time oil consumption measurement.

Torque is measured with a Kistler 4504B Torque Flange with a capacity of 2000 Nm and an accuracy of ± 0.05%. The torque flange is mounted in the driveline between the engine and the dyno absorber.

The Re-Sol RS 515A-125 Fuel Flow Measurement System utilizes a “float tank”-style level controller to combine the return fuel with the incoming fuel and reduce measurement to a single flow path. The measurement is done with a Micro Motion CMFS010 with an accuracy of ± 0.05% and a capacity of

110 kg/hr. The test cell instrumentation is calibrated on a quarterly basis, with the exception of emissions measurement, which is calibrated daily.

Performance and Emissions Test Results

The measured fuel consumption confirmed expectations for the development engine; combustion performance and pumping losses were in good agreement with predictions. The best point fuel consumption of 194.5g/kWh occurred at both A100 and B100 point, which equates 43.1% brake thermal efficiency. The best indicated efficiency of 52.3% occurred at C25 operating point. The SET 12 mode

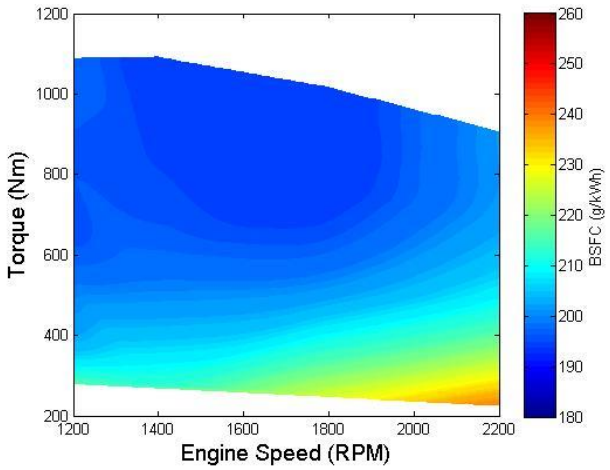

Figure 8: Multi-cylinder BSFC map

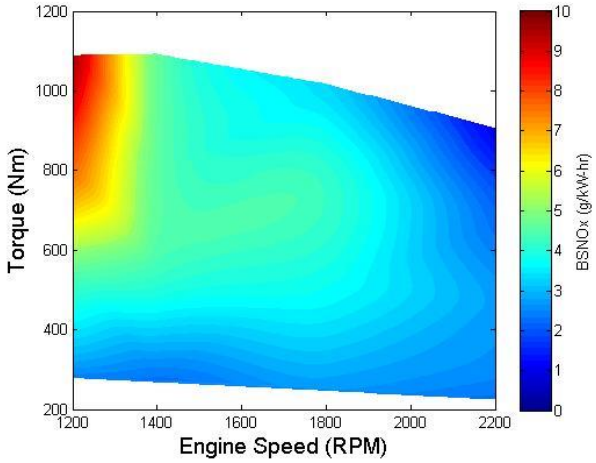

Figure 9: Multi-cylinder BSNOx map

weighted average fuel condition equates to 201.1 g/kWh. The 12 mode cycle measured BSNOx averages 3.30 g/kWh enabling tailpipe emission compliance US 2010 with typical SCR conversion efficiency. The NOx map (Figure 9) shows noticeable dependency with engine speed, which is a consequence of the speed dependency of the residual gas content during the uniflow scavenging process.

The 0.050g/kWh weighted average 12mode results of BS Soot (Figure 10) is in a good range not only to meet tailpipe emissions but also to achieve low particulate filter regeneration frequency. Slightly higher BSSoot emission is measured around C100 due to lower air mass than desired, future engine build are

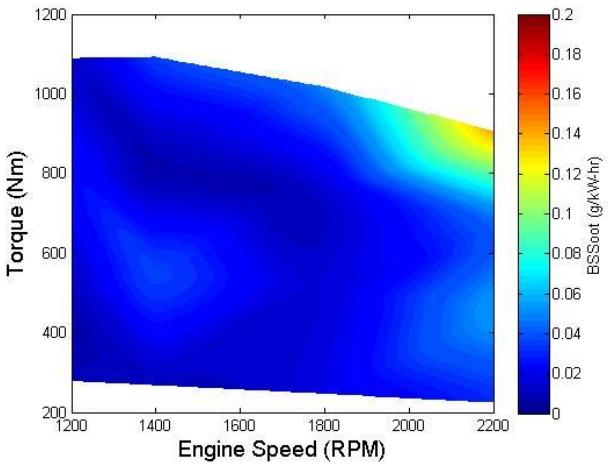

Figure 10: Multi-cylinder BSSoot (AVL415S) map

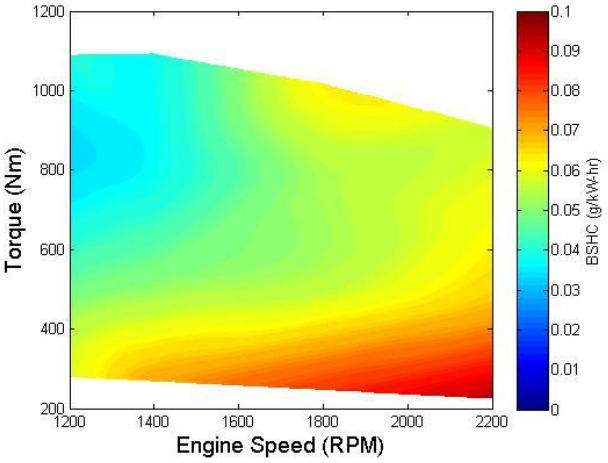

Figure 11: Multi-cylinder BSHC map

expected to perform better at that area.

The BSHC (shows in Figure 11) weighted average of 0.06 g/kWh is extremely low, does not even require any aftertreatment reduction.

Table below summaries the expected tailpipe emission with corresponding aftertreatment efficiencies.

	EPA 2010 Tailpipe limit [g/kWh]	Engine out measurement [g/kWh]	Aftertreatment conversion efficiency	Expected tailpipe emissions [g/kWh]
NOx	0.27	3.30	93% (SCR)	0.23
PM	0.013	0.050	99% (DPF)	0.001
HC	0.19	0.057	99% (DOC)	0.001

The low measured BSCO (shown in Figure 12) values across the entire map confirm the excellent quality of the combustion process of the proprietary Achates Power combustion system.

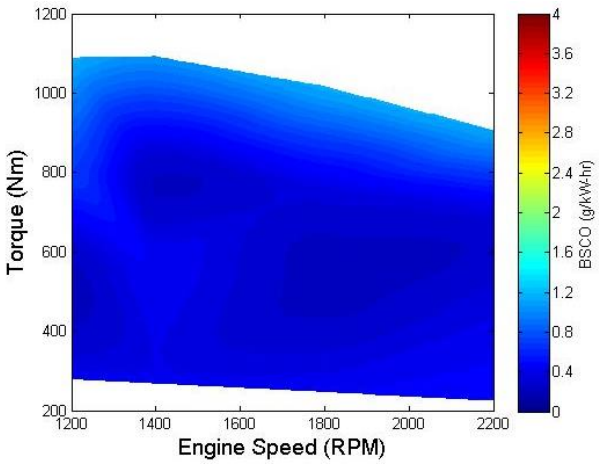

Figure 12: Multi-cylinder BSCO map

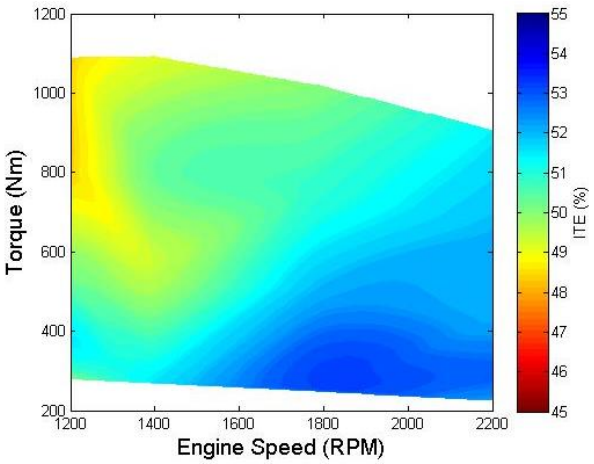

Figure 13: Multi-cylinder ITE map

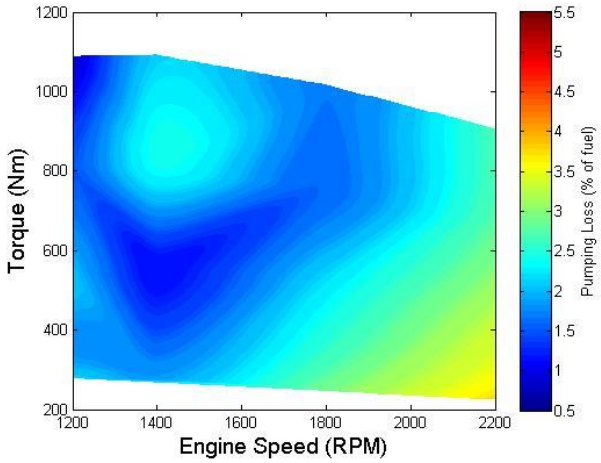

Figure 14: Multi-cylinder pumping loss map

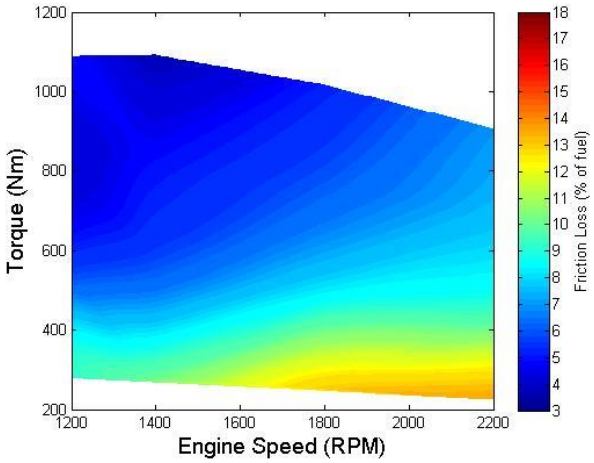

Figure 15: Multi-cylinder friction map

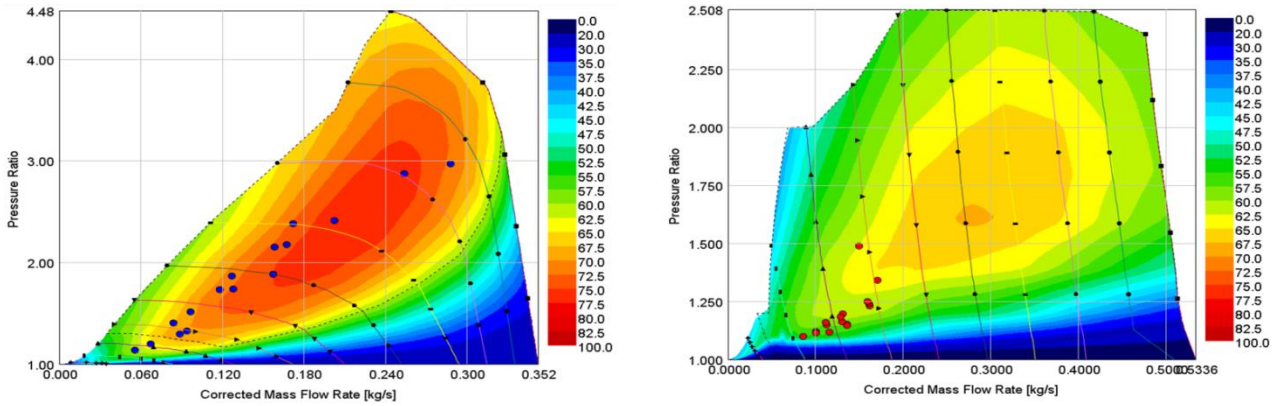

Figure 16: Turbocharger compressor (left) and supercharger map with operating points

Figure 16 shows the operating point on the turbocharger and supercharger compressor maps. Unlike typical four-stroke engines, the OP2S engine does not need as wide of a compressor map. Therefore, achieving good efficiency at rated power while still maintaining a good surge margin at peak torque and other low-speed, high-load points was not as difficult

Table 2 Selected SET 12 mode measurement data

Engine Condition		**A25**	**A75**	**A100**	**B50**	**B75**	**B100**	**C25**	**C75**	**C100**
Engine Speed	rpm	1400	1400	1400	1800	1800	1800	2200	2200	2200
IMEP	bar	4.6	12.3	15.9	8.1	11.5	15.1	4.3	10.8	14.3
BMEP	bar	3.5	10.5	13.9	6.5	9.7	13	2.8	8.6	11.6
Indicated Power	kW	52.7	141.2	182.3	120	169.5	222.5	77.1	194.2	258.2
Brake Power	kW	40.2	120.3	160.2	95.8	143.5	191.8	51.4	154.8	209.2
Indicated Thermal Efficiency	%fuel	51.6	50.3	49.2	52.1	50.9	50.1	52.3	52.01	51.46
Brake Thermal Efficiency	%fuel	39.3	42.8	43.1	41.5	43	43.1	34.8	41.4	41.6
Friction Loss	%fuel	10.4	5.1	4.0	8.3	6.3	5.3	13.7	7.8	7.1
Pumping Loss	%fuel	1.9	2.4	2.1	2.3	1.6	1.7	3.8	2.8	2.7
ISFC (Engine)	g/kWh	162.8	166.9	170.8	161.2	164.8	167.6	160.6	161.5	163.2
BSFC (Engine)	g/kWh	213.4	195.8	194.5	201.9	194.7	194.5	240.7	202.6	201.4
BSNOx	g/kWh	2.336	4.743	4.789	3.853	4.299	3.351	2.288	1.841	1.037
BSSOOT	g/kWh	0.013	0.011	0.036	0.017	0.017	0.05	0.032	2.276	1.218
BSCO	g/kWh	0.398	0.286	1.067	0.224	0.384	1.173	0.527	0.325	1.154
BSHC	g/kWh	0.071	0.038	0.038	0.056	0.054	0.063	0.094	0.062	0.058
Peak Cylinder Pressure	bar	79	162	198	129	161	197	90	173	200
50% Mass Burned Fraction	deg aMV	2.7	3.1	3	2	2.7	4	0.3	1.6	4.6
Burn Duration 10-90%	deg	15.7	27.8	31.1	21.4	22.6	25.0	18.7	21.8	22.0
Air/Fuel Ratio	-	30.2	27.3	24.4	28.9	23.9	22.1	30.9	24.4	21.3
External EGR Rate	%	32.3	31.5	30.2	27.6	25.6	26.0	32.0	33.2	34.0
Intake Manifold Pressure	bar	1.338	2.297	2.705	2.034	2.420	2.989	1.593	2.730	3.305
Intake Manifold Temperature	degC	38	40	43	40	40	44	39	40	45
Turbine Outlet Temperature	degC	250	278	311	264	323	343	240	287	327

Multi-Cylinder Engine Modelling

The first portion of this paper has discussed initial results from a multi-cylinder engine built for research and development purposes. A production intent 4.9L engine targeted for 2017+ release will include improvements in combustion, pumping and friction.

GT-Power, a capable one-dimensional engine and vehicle simulation tool, is used to predict what the performance of such an engine would be.

A two-step approach is used in making future multi-cylinder predictions from current 4.9L multi-cylinder measurements. The first step is a correlating the 1-D model to test cell measurements. This allows for accurate determination of in-cylinder heat transfer, trapped composition, friction losses and pumping losses. Step two involves assessing what model changes and assumptions will be necessary to make the proper prediction on 4.9L engine, than apply those on a 11L engine to predict a heavy duty engine performance.

The 1-D model requires a detailed characterization of the scavenging process because it is important to arrive at the correct concentrations of fresh air and residual gas in the cylinder prior to the start of the closed-cycle portion of the simulation. For this reason, the scavenging efficiency was measured in the test engine using an in-cylinder CO2 sampling method, and the scavenging efficiency versus scavenge ratio relationship was used in both the correlation and prediction process.

Before accurate correlation can begin, the friction and engine accessory efficiencies are measured with dedicated tests and then input into the 1-D model. The multi-cylinder model air-handling system consists of a supercharger, a turbocharger, a charge air cooler after each compression stage and EGR coolers. The size and characteristics of the air-handling system components are application specific. The compressor and turbine is modeled using map data provided by a turbocharger supplier, and the supercharger model uses a full map obtained from a supercharger supplier.

In the correlation model, the combustion chamber geometry, the piston motion and the porting profiles are identical to what exists in the multi-cylinder engine. Engine speed, fuel flow rate, air flow rate, EGR percentage, cylinder pressures at 30° before minimum volume, brake torque, and the intake/exhaust manifold and compressor inlet/turbine outlet pressures and temperatures match the measured values. The rate of heat release is derived from the measured cylinder pressure and is input directly into the combustion sub-model. From this, the trapped conditions in the cylinder are determined as well as the in-cylinder heat transfer coefficient using the measured indicated thermal efficiency as a target. The model is iterated until cylinder pressure traces, crank angle resolved intake and exhaust pressures, air system pressure drops and temperatures, and turbo machinery performance matches the measured values. Once the model has been fully correlated over the entire operating range, it is then transformed into the prediction model. This is accomplished by fixing the in-cylinder heat transfer coefficient and controlling fuel flow with a brake mean effective pressure (BMEP) controller. Hardware changes, identified improvements in component performance, or certain calibration changes can be applied to this model to predict how overall engine performance and losses change as a result of the given change. Modifications can be performed one at a time to determine individual performance gains or all at once to find the effects of a full engine upgrade.

Model Correlation

3D Gas Exchange Modeling

CFD model of the A48-3-16 engine air system was created to model the gas exchange process. The domain starts after the supercharge bypass and ends at the EGR pickup and turbo inlet. The model contains six moving pistons that cover and uncover the intake and exhaust ports and intake and exhaust manifolds. Upstream and downstream pipes were also included to accurately predict pressure wave dynamics in the system. The simulations were run using CONVERGE 2.1 with moving boundaries. Boundary conditions are obtained from 1D GT-Power complete engine model simulations at different engine loads and speeds. The simulation tracks residual gases and fresh air charge in all three cylinders to predict Delivery Ratio (DR), Trapping Efficiency (TE), Scavenging Efficiency (SE) and Charging Efficiency (CE).

The A48-3-16 engine is equipped with high-speed pressure measurements at the intake and exhaust manifolds. A hot wire anemometer and a laminar flow element are used to measure mass flow rate per cycle in the engine at the test cell. With these measurements it is possible to validate the CFD simulation results.

Figure 18 begins at 120° crank angle, which is minimum volume for Cylinder 2. The comparison shows very good correlation between predicted and measured pressure waves in both intake and exhaust manifolds.

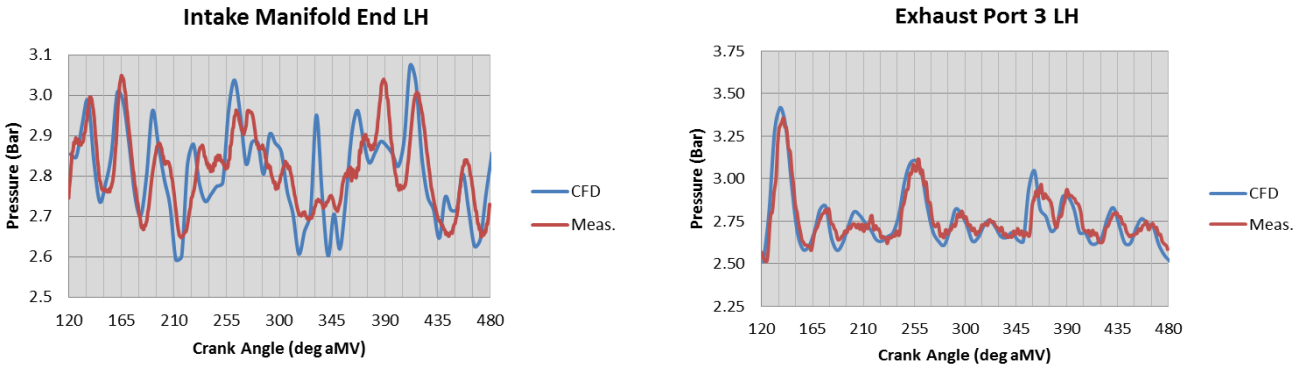

Figure 17: Intake and exhaust pressure correlation

Correct prediction of the pressure wave dynamics is essential to have a good delivered mass correlation. At 1800 rpm and a 50% load point, the measured delivered mass per cycle was 9043.3 mg/cycle where CFD simulation predicts 8876.7 mg/cycle. The difference in measured and predicted delivered mass per cycle is below 2%.

Good correlation is critical to build confidence in the simulation methodology and results. With this confidence, many virtual prototypes can be tested in a short period of time to help choose an optimal design early in the engine design phases.

3D Combustion System Modeling

Commercially available CONVERGE CFD software [14, 15] is used to perform in-cylinder simulations of the OP2S combustion system. CONVERGE offers detailed chemistry solvers along with hydrodynamic solvers that provide a basis of combustion simulation. The methodology, adopted for in-cylinder combustion simulation, is a combination of multi-cylinder engine (MCE) air flow simulation as described in the previous sub-section and coupling the MCE air flow results with in-cylinder combustion simulation for only one cylinder. In the present study, the cylinder towards the end of the intake manifold (namely Cylinder 3) is chosen as a representative cylinder for simulation purposes. Because of its extreme location away from the inlet of the intake manifold, Cylinder 3 is a good choice of representation to improve combustion using hardware changes, such as injector hole size, spray patterns, port orientation, etc. For any hardware changes in Cylinder 3 that result in improved combustion, similar improvements are also observed in other cylinders. Intake and exhaust port geometries are not included as only the closed portion of the cycle from exhaust port closing (EPC) (= -118 degree aMV) to exhaust port opening (=114.5 degree aMV) is simulated for the purpose of combustion analysis. This is computationally efficient compared to simulating an entire multi-cylinder with detailed chemistry solvers. The initial conditions for the simulation require trapped thermodynamic conditions and trapped flow conditions. Trapped flow conditions include the velocity field, turbulent kinetic energy and dissipation rate, which are obtained from the entire MCE gas-exchange simulation as described in the previous subsection. The trapped pressure is specified based on the cylinder pressure measurements, and the trapped composition and temperature are obtained from a two-zone mixing model based on scavenging measurements. Note that trapped composition and temperature can also be obtained using well-correlated, one-dimensional code, such as GT-Power, that simulates a multi-cylinder engine with imposed combustion characteristics. In the case of the Achates Power engine, the scavenging measurements provide direct means of deriving trapped composition and temperature.

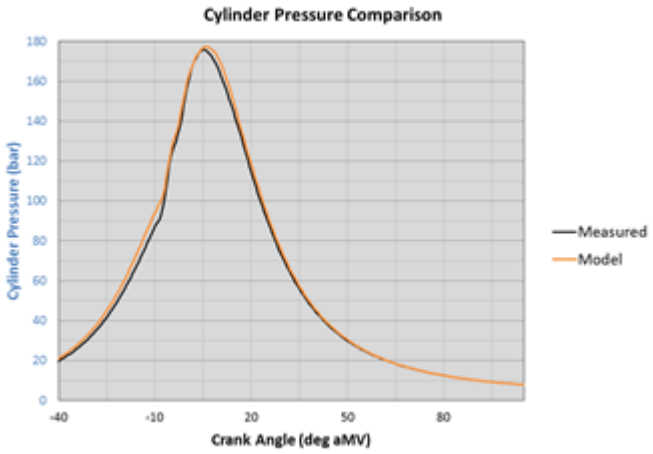

Figure 18: Comparison of measured and model cylinder pressure curves at B75

A detailed chemistry model involving a well-known reduced chemistry mechanism for n-heptane (diesel fuel surrogate) with 35 species and 77 reaction steps [16], which include a NOx sub-mechanism, is used. Soot emissions are modeled using a two-step model, which includes a Hiroyasu formation step with acetylene as the precursor [17], and an oxidation step involving carbon oxidation by O2 molecules

[18]. Sprays are modeled using a modified KH-RT break-up model without the use of an ad-hoc breakup length [15, 19] and the O'Rourke collision model [15, 20], whereas turbulence is modeled using the RNG k-ε model [15, 21]. Fuel injection rate profiles are specified based on measured data from a state-of-the-art, in-house fuel laboratory with IFR (Injection Flow and Rate) capabilities [22]. Example of the archived correlation at B75 point is shown in Figure 19.

Performance and Emissions Roadmap

The Achates Power opposed-piston, two-stroke engine has demonstrated a cycle weighted average brake thermal efficiency (BTE) of 41.8% with engine hardware and calibration that are still in an early stage of development. Higher engine thermal efficiencies will be achieved through hardware and calibration improvements, some of which are unique to the Achates Power engine architecture and some of which are industry-wide advancements. To quantify the effect of these possible improvements, a BTE roadmap has been developed. The potential efficiency improvements are estimated based on internal analysis as well as findings from a report on fuel economy technologies to the United States National Academy of Sciences. Figure 19 shows the energy balance and efficiency improvements using the 12-mode weighted average results. The predicted brake-specific fuel consumption map is also shown in Figure 20.

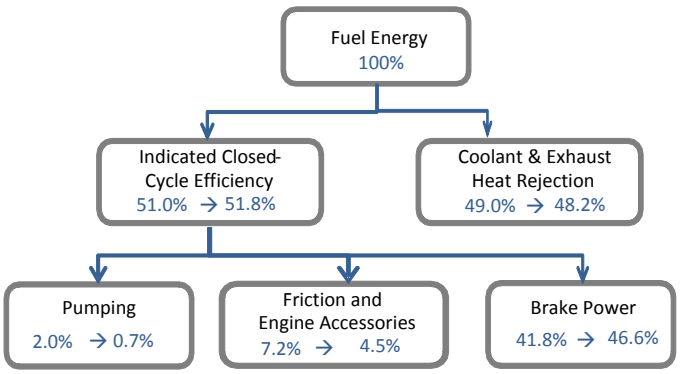

Figure 19: Energy balance and efficiency improvements of cycle-weighted average

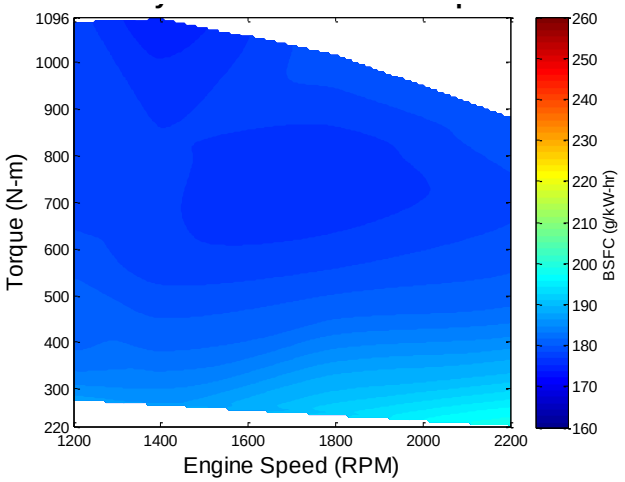

Figure 201: A48-3-16 brake-specific fuel consumption roadmap prediction for 2017+

In order to achieve a cycle-weighted brake thermal efficiency of 46.6% or 180g/kWh BSFC, the indicated closed-cycle efficiency, pumping work, mechanical friction and the power consumption of the engine accessories all require further improvements. A detailed discussion of each improvement opportunity can be found in the following sections to support the quantitative estimates put forth in Figure 19.

Combustion improvements

The ability to convert fuel energy to mechanical energy efficiently and cleanly while still meeting external mechanical and emission constraints is paramount to a successful internal combustion engine. For the current weighted average, a gross indicated thermal efficiency of 51.0% is achieved using a calibration with a maximum of 10 bar/deg maximum pressure rise rate, and a greater than 90% efficient SCR device that allows 2010 U.S. emissions requirements to be met with 3.3 g/kW-hr engine-out NOx.

Improving the combustion system is a primary step toward increasing the brake thermal efficiency. In the present analysis, the effects of changes to the designed engine hardware and calibration on indicated thermal efficiency were evaluated using CFD results, new piston bowl shapes were developed, fuel injector nozzle configurations were designed to more favorable heat transfer and combustion characteristic. The cylinder port design also can be improve scavenging performance. The new piston bowl and nozzle design resulted in a 0.7%$_{fuel}$ improvement over the current status.

Gas Exchange

Gas exchange losses for a two-stroke engine are represented by the pumping work provided by the crankshaft-driven supercharger. The mechanical losses to drive the supercharger are included in the accessory power consumption and will be discussed in the next section. In general, the supercharger power requirements depend on the pressure losses of the entire air system, the additional pumping to compensate for short-circuiting of fresh air during scavenging, the EGR rate and the efficiencies of the supercharger and turbocharger. All of these effects were quantified by a 1D engine performance simulation tool. The baseline is the measurement indicated pumping losses, equivalent to 2.0%$_{fuel}$.

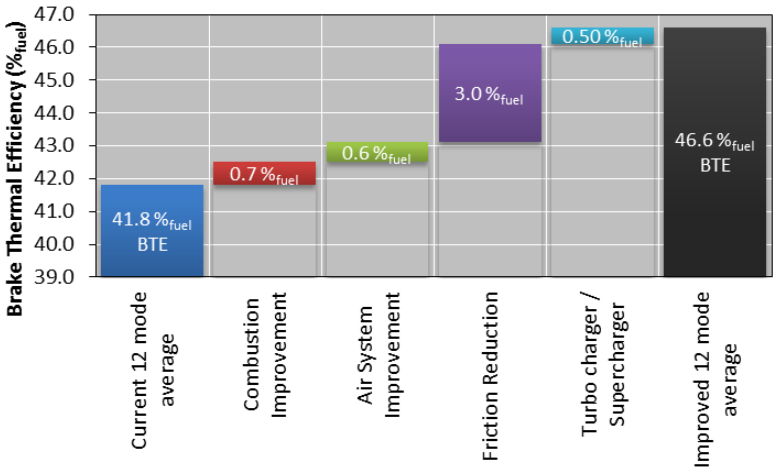

Figure 21: Contributors of BTE improvements of cycle-weighted average

Several measures were applied in succession to reduce the pumping work. First, the porting arrangement was optimized for the future hardware. Secondly the intake system was modified allowing more efficient air induction, reducing pressure drop. These design differences were modeled in CFD to quantify the scavenging improvements over the design currently under testing. Thirdly more efficient charge air cooler were modeled, allowing the total system pressure to be reduced while increasing the trapped air-fuel ratio. The 1D simulation model determined 0.6%$_{fuel}$ as a results of all these improvements.

As Achates Power moves to a 2017 production-intent engine configuration, supercharger suppliers will be able to produce a unit that is better suited for the opposed-piston, two-stroke diesel engine as opposed to the high pressure ratio superchargers currently used on four-stroke engines. With current technology, the Achates Power opposed-piston engine utilizes a very small portion of the available supercharger maps that is outside of the maximum efficiency island (see Figure 16, supercharger map). By designing a unit that focuses on higher efficiency in the low speed, low pressure ratio portion of the map, pumping work will be reduced. Finally, all of these advancements in pumping efficiency will pro-

vide the opportunity to match a different turbocharger. Higher exhaust temperatures, improved supercharger pumping, and future improvements in turbocharger technology help to improve turbocharger efficiency. The improvement with a supercharger better suited for opposed-piston, two-stroke diesel and better turbocharger matches provide0.5%$_{fuel}$ improvements.

All of these advances drop pumping losses down to 0.7%$_{fuel}$ as shown in Figure 19.

Friction and Engine Accessories

The power cylinder friction (ring/liner and piston/liner friction) closely matches the situation in a four-stroke diesel engine, since both engine types employ a slider-crank mechanism. It is, therefore, a reasonable strategy to leverage the same industry-wide advancements in the area of tribology and advanced lubricants to lower the friction losses of the power cylinder in an opposed-piston engine. For this roadmap, the friction reduction for the power cylinder, bearings and geartrain are projected to divide up as follows: 0.35%$_{fuel}$ are gained from the power cylinder based on further optimization of the ring and piston skirt contours combined with advanced surface textures and/or coatings; 0.87%$_{fuel}$ from the main and rod bearings based on size optimization and oil temperature management; and 0.94%$_{fuel}$ from the geartrain based on optimized geartrain design and lastly the lower lube pump power requirement allows 0.84%$_{fuel}$ reduction. Combined, the projected improvements is 3%$_{fuel}$, which highlights the improvement potential starting from a robust oversized design such as Achates Power A48-3-16 development engine. It is important to note that some previously introduced improvement actually increase the friction, hence more reduction is required to achieve 46.6% cycle weighted BTE than Figure 19 suggests.

By incorporating all friction reduction measures, the friction losses reduce to 4.5%$_{fuel}$.

Heavy Duty Engine Prediction

Previous section detailed the currently achieved engine performance and emission results, as well the road map to achieve 46.6% weighted cycle average brake thermal efficiency representative of a volume production medium duty engine design. Using the 4.9L multi cylinder engine correlated models a heavy duty engine model was created.

Table 3: Heavy duty engine specification

HD engine specification	
Displacement	11.0 L
Arrangement, # of Cyl.	Inline 3
Bore	125 mm
Total Stroke	300 mm
Stroke-to-Bore Ratio	2.4
Compression Ratio	15:01
Nominal Power (kW@rpm)	390 @ 1700-2100
Max. Torque (Nm@rpm)	2200 @ 1200-1600

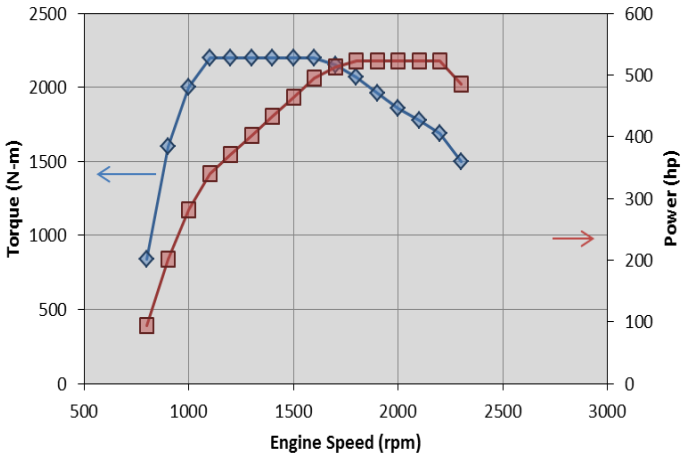

Figure 22: Heavy duty engine power and torque curve

Completive power and torque target were selected in this category (Table3 and Figure 22).

All improvement potential described in previous section was applied to create a BSFC map representative for much larger bore engine. The stroke to bore ratio was increased to 2.4 from 2.2 of the 4.9L engine in order to improve area to volume ratio and also improve gas-exchange characteristics over the 4.9L engine. Engine calibration was assumed to reach similar engine out emission level as of 4.9L engine. The combustion system was scaled from 98.4mm bore to 125mm bore size. The more favorable area to volume ratio and the lower in-cylinder heat transfer allow reaching higher brake thermal efficiencies shown in Figure 23; the prediction shows 51.5% best point brake thermal efficiency can be achieved, which equates 162.7 g/kWh BSFC at A75 point. The SET 12 mode weighted cycle average fuel consumption is calculated 166g/kWh, brake thermal efficiency of 50.5%.

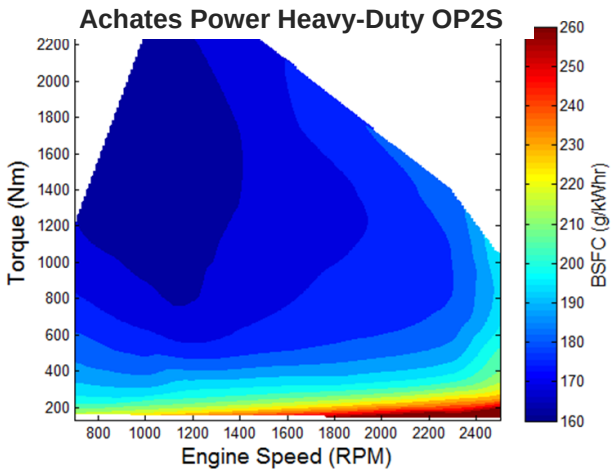

Figure 23: 11L Heavy duty engine BSFC map predicted for 2017+

Engine Vibration

The inherent vibration characteristics are an important consideration when evaluating engine architectures for any on-road application. The current heavy- and medium-duty market is dominated by inline six-cylinder, four-stroke engines. This baseline configuration features theoretically “perfect” force and moment balancing, with the only residual effect being the reaction from the engine output torque. Therefore, any un-cancelled residual forces or moments from the opposed-piston, two-stroke, three-cylinder engine will be an additional input to the engine mount system design.

The engine output torque reaction moments will be comparable to an inline six-cylinder, four-stroke engine with the same crank rotational speed and mean brake torque. This is because the frequency of the firing events is the same between both cases. The other assumptions in this statement are that the rotational inertias and peak cylinder pressures of the systems are comparable.

The opposed-piston architecture inherently balances out the majority of the piston acceleration forces within each cylinder. As the intake side piston decelerates towards the injector plane, the exhaust side piston also decelerates in a similar magnitude, but in the opposite direction. The only offset is a result of the phase shift between the two pistons. The exhaust piston is phased slightly ahead of the intake piston

to maintain favorable intake to exhaust port time-areas and overall expansion ratio. As a result, there is a small residual piston inertial force from each cylinder.

The firing order for a three-cylinder, opposed-piston, two-stroke (OP2S) features even 120° firing events. When the residual force from one pair of pistons is at a maximum, the residual forces from the other two pairs of pistons are half of the magnitude each, and in the opposite direction relative to the first. This means that the forces effectively cancel out. To confirm this, a kinematic model was created in CREO/Mechanism. The system analysed was the A48-3-16 research engine at an 8° exhaust crank lead, operating at peak power.

The mechanism analysis was configured to output the residual forces and moments, neglecting component compliance and system resonances. The residual block forces are shown in Figure 24. The magnitudes of these residual forces are exceptionally small, and may be neglected for any engine mount design.

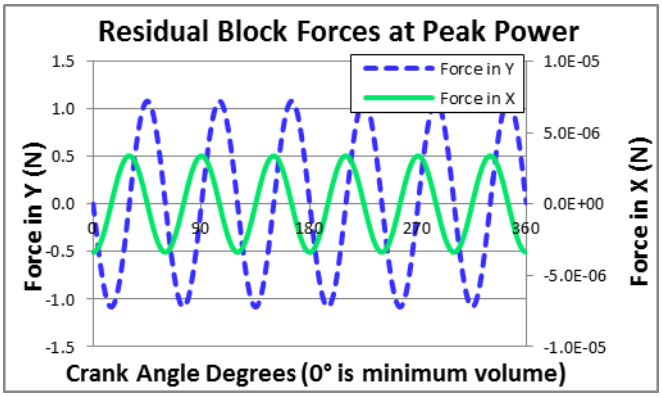

Figure 24: Residual block forces at peak power

Since the internal forces essentially cancel, and the torque reaction moments are comparable, the moments about the X and Y axes are the last excitations to consider. The output from the mechanism model resulted in the moments shown in Figure 25.

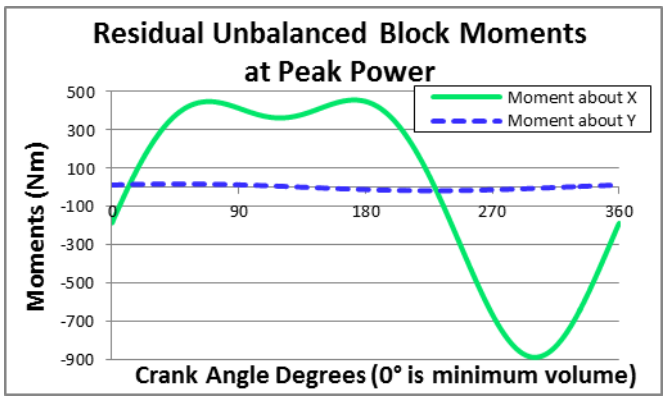

Figure 25: Residual unbalanced block moments at peak power

Moment magnitudes in this range are well within standard engine mount design capability. This characteristic curve features both first- and third-order content. Since the first-order content magnitude exceeds the third-order content, there is an opportunity to reduce the peak even below this reasonably low level. Adding equal and opposite masses to the end of one crank (or any shaft rotating at crank speed) will

counteract the moment about the X-axis without generating any residual forces. There will be a first order sine wave added to the residual moments about the Y-axis as a result of this balancing.

Again, the CREO/Mechanism model was used to demonstrate this concept. The results are shown in Figure 26.The mass and eccentricity of the "balancing" feature was increased until the peak magnitude of the moments about the Y axis approached the peak magnitude of the moments about the X axis. Of course, if the particular mounting system design isolates the moments in either the X- or Y-axis more effectively than the other, this peak moment about the X-axis reduction technique may be adjusted.

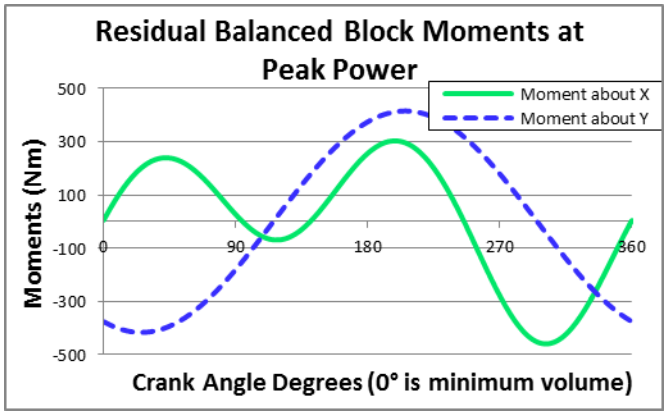

Figure 26: Residual balanced block moments at peak power

The behaviour of the system trends increase the peak moments as a function of the square of the engine speed, and as a linear function of the exhaust crank lead. For example, this 8° exhaust crank lead results in a peak magnitude for the moment about X of less than 460 Nm. If the exhaust crank lead was reduced to 6°, the peak magnitude for the moment about X would be less than 345 Nm at the same engine speed.

Summary/Conclusions

- Achates Power is pleased to publish the first fully autonomous opposed-piston engine brake results, including fuel consumption and emissions.
- The performance demonstrated there is achieved with all the engine accessories and auxiliaries driven by the engine and without applying the latest developments that would be applicable to the opposed-piston engine, such as waste heat recovery, low friction coatings, thermal barrier coatings, electrified accessories, two-stage turbochargers and turbo-compound.
- The technologies that Achates Power has developed for the opposed-piston engine have demonstrated the ability to exceed any four-stroke engine of equivalent size.
- The measured results shown in this paper are from a very initial attempt at demonstrating multi-cylinder brake performance. The significant learnings from this exercise will be the basis for continued further improvements leading to a potential cycle average fuel economy over the 12-mode points for 46.6% BTE on 4.9L engine size, while same technologies applied on 11.0L heavy duty engine the potential cycle average fuel economy over the 12-mode points is 50.5% BTE.
- This paper also describes how the Achates Power engine can be configured to be compact, light and easy to integrate in a vehicle.

-

References

1. DieselNet, Diesel Exhaust Emissions Standards, Retrieved from http://www.dieselnet.com/standards/.
2. Flint, M. and Pirault, J.P., "Opposed Piston Engines: Evolution, Use, and Future Applications", SAE International, Warrendale, PA ISBN 978-0-7680-1800-4, 2009.
3. Herold, R., Wahl, M., Regner, G., Lemke, J., and Foster, D., "Thermodynamic Benefits of Opposed-Piston Two-Stroke Engines," SAE Technical Paper 2011-01-2216, 2011, doi: 10.4271/2011-01-2216.
4. Regner, G., Naik, S., "Not All Two-Stroke Engines Are Created Equal", Retrieved from http://www.achatespower.com/diesel-engine-blog/2013/09/27/not-all-two-stroke-engines-are-created-equal/, 2013.
5. Regner, G., "Turbocharger Efficiency: An Underappreciated OP2S Advantage", Retrieved from http://www.achatespower.com/diesel-engine-blog/2013/01/23/turbocharger-efficiency/, 2013.
6. Regner, G., "The Achates Power Engine: Low NOx and Superior Efficiency", Retrieved from http://www.achatespower.com/diesel-engine-blog/2013/02/27/low-nox/, 2013.
7. Fuqua, K., Redon, F., Shen, H., Wahl, M., and Lenski, B., "Combustion Chamber Constructions for Opposed-Piston Engines", U.S. Patent Application US20110271932.
8. Venugopal, R., Abani, N., MacKenzie, R., "Effects of Injection Pattern Design on Piston Thermal Management in an Opposed-Piston Two-Stroke Engine", SAE International Technical Paper 2013-01-2423, 2013, doi:10.4271/2013-01-2423.
9. Regner, G., Fromm, L., Johnson, D., Koszewnik, J., Dion, E., Redon, F., "Modernizing the Opposed-Piston, Two-Stroke Engine for Clean, Efficient Transportation", SAE International Technical Paper 2013-26-0114, 2013, doi:10.4271/2013-26-0114.
10. Pohorelsky, L., Brynych, P., Macek, J., Vallaude, P., Ricaud, J., Obsernesser, P., Tribotté, P., "Air System Conception for a Downsized Two-Stroke Diesel Engine", SAE International Technical Paper 2012-01-0831, 2012, doi:10.4271/2012-01-0831.
11. Ostrowski, G., Neely, G., Chadwell, C., Mehta, D., Wetzel, P., "Downspeeding and Supercharging a Diesel Passenger Car for Increased Fuel Economy", SAE International Technical Paper 2012-01-0704, 2012.
12. Kalebjian, C., Redon, F., and Wahl, M. "Low Emissions and Rapid Catalyst Light-Off Capability for Upcoming Emissions Regulations with an Opposed-Piston, Two-Stroke Diesel Engine", Emissions 2012 Conference.
13. Teng, H. and Regner, G., "Characteristics of Soot Deposits in EGR Coolers", SAE International Journal of Fuels and Lubricants, Vol. 2, No. 2, pp. 81-90, 2010. Also published as SAE Technical Paper 2009-01-2671, 2009, doi:10.4271/2012-01-0704.
14. Senecal, P.K., Richards, K.J., Pomraning, E., Yang, T., Dai, M.Z., McDavid, R.M., Patterson, M.A., Hou, S., and Shethaji, T., "A New Parallel Cut-Cell Cartesian CFD Code for Rapid Grid Generation Applied to In-Cylinder Diesel Engine Simulations," SAE Paper No. 2007-01-0159, 2007.
15. Richards, K.J., Senecal, P.K., Pomraning, E., "CONVERGE (Version 1.4.1)," Convergent Science Inc., Middleton, WI, 2012.
16. Patel, A., Kong, S., -C., and Reitz, R.D., "Development and Validation of a Reduced Reaction Mechanism for HCCI Engine Simulations," SAE Technical Paper 2004-01-0558, 2004.
17. Hiroyasu, H., and Kadota, T., "Models for Combustion and Formation of Nitric Oxide and Soot in DI Diesel Engines," SAE Paper No. 760129, 1976.
18. Nagle, J., and Strickland-Constable, R.F., "Oxidation of Carbon Between 1000-2000 C," Proceedings of the Fifth Carbon Conference, Vol. 1, p.154, 1962.
19. Patterson, M.A., "Modeling the Effects of Fuel Injection Characteristics on Diesel Combustion and Emissions," Ph.D. Thesis, University of Wisconsin-Madison, 1997.
20. O'Rourke, P.J., "Collective Drop Effects on Vaporizing Liquid Sprays," Ph.D. Thesis, Princeton University, 1981.
21. Han, Z., and Reitz, R.D., "Turbulence Modeling of Internal Combustion Engines Using RNG k-ε Models," Combustion Science and Technology, Vol. 106, 1995.
22. Klyza, C., "Optical Measurement Methods used in Calibration and Validation of Modeled Injection Spray Characteristics," Poster P7, presented in the 2010 Directions in Engine-Efficiency and Emissions Research (DEER) Conference.
23. Delgado, o and Lutsey, N., The U.S. SuperTruck program expediting the development of advanced heavy-duty vehicle efficiency technologies, International Council on Clean Transportation, 2014

Contact Information

Gerhard Regner
Vice President, Performance and Emission
Achates Power, Inc.
Email Address: regner@achatespower.com